

## Molecular-dynamics simulation of pressure broadening of sodium resonance line by argon

G. J. Erickson and K. M. Sando

*Department of Chemistry, University of Iowa, Iowa City, Iowa 52242*

(Received 22 April 1980)

A molecular-dynamics simulation of the pressure broadening of the sodium resonance line by argon gives an absorption line shape which is compared to results from the Anderson-Talman classical path theory. The system consists of 255 argon atoms and one sodium atom in a box with periodic boundary conditions. The size of the box and the initial velocities are chosen to correspond to a particle density of  $2 \times 10^{21} \text{ cm}^{-3}$  and a temperature of 450 K. The time-dependent difference potential matrix is utilized in an adiabatic approximation to give the molecular-dynamics line shape. Spin-orbit coupling and Doppler broadening are neglected. A Fourier-transform technique is used to evaluate the Anderson-Talman theory line shape for the same system. Remarkable agreement is found between the molecular-dynamics line shape and the line shape obtained from the one-perturber spectrum by means of the Anderson-Talman theory. Comparison of molecular-dynamics line shapes calculated with a scalar and with a vector dipole transition moment shows that relaxation of polarization has a significant broadening effect on the center of the line.

### I. INTRODUCTION

In the theory of pressure broadening of atomic spectral lines,<sup>1,2</sup> the line shape is related to few-body interactions among the atoms. The quantitative reliability of the various physical assumptions made to simplify the theory has not been thoroughly tested because tests based upon a comparison of calculated and observed line shapes are inconclusive when the interatomic potentials are imprecisely known.

The technique of molecular-dynamics simulation<sup>3</sup> can be used to generate "experimental" data for a system with known interactions. In this computer-simulation technique, a finite system is allowed to evolve with time and properties of interest, such as an atomic line shape, calculated from the detailed dynamics of the particles. Approximations in the dynamics, such as pairwise additivity of forces and a classical path, are usually made.<sup>4</sup>

In this work, molecular-dynamics data for the sodium resonance line in absorption pressure broadened by argon are analyzed to give an atomic line shape using methods that are based upon an adiabatic approximation to the difference potential (discussed in Sec. II). The feasibility of producing atomic line shapes with an acceptable statistical error is proved and the importance of perturber-perturber interactions and rotation of polarization axis on the line shape are assessed. Comparisons are made with theories based upon the concepts of Jablonski<sup>5</sup> and Anderson<sup>6</sup> that the  $N$ -perturber line shape can be expressed in terms of convolutions of one-perturber line shapes, or alternatively, the  $N$ -perturber autocorrelation function can be expressed in terms of products of one-perturber autocorrelation functions.

Successful completion of this work required development of new numerical methods for analysis of the molecular-dynamics data and for application of the classical path Anderson-Talman theory. These methods are described in Secs. III and IV. The results are presented in Sec. V and discussed in Sec. VI.

### II. DIFFERENCE POTENTIAL

The sodium resonance line results from a transition from the spherically symmetric ground  $3^2S$  state to the manifold of  $3^2P$  states. Under conditions in which the sodium atom density is much less than the argon atom density, the pressure broadening of the spectral line is due to sodium-argon interactions with a negligible contribution from sodium-sodium interactions. In the classical path approximation (see following sections) the line shape is then directly related to the difference in the interactions of argon atoms with  $^2P$  and with  $^2S$  sodium atoms.

The interaction of a  $^2S$  sodium atom with an assembly of argon atoms is obtained quite simply and with reasonable accuracy by making the Born-Oppenheimer and pairwise additivity approximations. The total interaction energy as a function of the positions of the atoms is given by

$$V_S = \sum_i V_X(R_i) + \sum_{i < j} V_{Ar}(R_{ij}), \quad (1)$$

where  $V_X$  is the diatomic interaction potential between a sodium atom and an argon atom in the ground  $X^2\Sigma$  state,  $R_i$  is the distance between the sodium atom and argon atom  $i$ ,  $V_{Ar}$  is the interaction potential between argon atoms  $i$  and  $j$ , and the sums run over argon atoms. In the molecular-dynamics simulation of an absorption experiment,

the motion of the atoms is governed by forces derived from this ground-state potential energy surface.

The interaction of a  $^2P$  sodium atom with an assembly of argon atoms is complicated by the degeneracy of the  $^2P$  states. The spin-orbit interaction causes the resonance line to break up into a doublet at low pressures; it causes broadening at intermediate pressures, but at the very high pressure used here its effect is negligible, thus we simplify the system by neglecting the spin-orbit interaction. Then, because there is only one unpaired electron in the system, and we consider only electric-dipole transitions, the electron spin does not influence the spectrum. With this simplification, the  $^2P$  configuration includes three degenerate states corresponding to the three values of the orbital angular momentum projection. In a previous publication<sup>7</sup> it was shown that the interaction potential can then be considered to be pairwise additive as a  $3 \times 3$  matrix

$$\underline{V}_P = \bar{V} \cdot \underline{1} + \underline{G}, \quad (2)$$

where

$$\bar{V} = \sum_i \frac{V_\Sigma(R_i) + V_\Pi(R_i)}{2} + \sum_{i < j} V_{Ar}(R_{ij}) \quad (3)$$

and

$$\underline{G} = \sum_i \frac{V_\Sigma(R_i) - V_\Pi(R_i)}{2R_i^2} \underline{\Delta}(\vec{R}_i). \quad (4)$$

The functions  $V_\Sigma$  and  $V_\Pi$  are Born-Oppenheimer interaction potentials in the  $B^2\Sigma$  and  $A^2\Pi$  diatomic states,  $\vec{R}_i$  is the distance vector from the sodium atom to perturber  $i$ , and in the  $\{p_x, p_y, p_z\}$  representation  $\underline{\Delta}(\vec{R}_i)$  is the real matrix

$$\underline{\Delta}(\vec{R}_i) = \begin{pmatrix} x_i^2 - y_i^2 - z_i^2 & 2x_i y_i & 2x_i z_i \\ 2x_i y_i & y_i^2 - x_i^2 - z_i^2 & 2y_i z_i \\ -2x_i z_i & 2y_i z_i & z_i^2 - x_i^2 - y_i^2 \end{pmatrix}, \quad (5)$$

where  $x_i$ ,  $y_i$ , and  $z_i$  are the Cartesian components of  $\vec{R}_i$ . The difference potential matrix is given by

$$\underline{\Delta V} = \underline{V}_P - V_S \cdot \underline{1}. \quad (6)$$

The perturber-perturber interactions cancel in the difference potential.

Because of the three-fold degeneracy of the sodium atom  $^2P$  configuration, there are three adiabatic excited states of the polyatomic system (sodium atom plus argon atoms). The eigenvalues of the difference potential at each geometric configuration of the system define three difference potential surfaces which correspond to the three adiabatic excited states. We use these surfaces in analyzing the molecular-dynamics data, and in this sense we utilize an "adiabatic approximation."

The three components of each eigenvector of the potential matrix give the direction cosines of the transition moment vector for the corresponding state

$$\vec{\mu}_j = |\mu| \sum_i D_{ij} \hat{e}_i, \quad (7)$$

where  $\hat{e}_1$ ,  $\hat{e}_2$ , and  $\hat{e}_3$  are unit vectors in the  $x$ ,  $y$ , and  $z$  directions,  $D_{ij}$  is the  $i$ th component of eigenvector  $j$ , and  $|\mu|$  is the magnitude of the atomic transition moment, which will be assumed independent of the configuration of perturbers.

### III. MOLECULAR-DYNAMICS METHOD

In the molecular-dynamics simulation, 255 argon atoms and one sodium atom are given initial positions and velocities within a box with periodic boundary conditions, after which they are allowed to move according to Newton's equations of motion. Initial velocities are chosen to have a mean square value corresponding to the desired temperature, but are otherwise random. Initial positions are at the sites of a face-centered cubic lattice. The size of the box is determined by the desired number density. An absorption experiment was simulated in the sense that the dynamics was carried out on the ground-state potential energy surface, for which pairwise additivity was assumed.

In the molecular-dynamics algorithm, the box is divided into cubical cells of edge length equal to the "range of the interactions." We chose 125 cells of edge length 19.05 bohr, at which distance the potentials were arbitrarily truncated. Distances (squared) between particles within the same cell and in adjacent cells are calculated. A linked-list technique<sup>8</sup> is used to follow the cell location of each particle. All pair interactions are interpolated by means of a tension-spline algorithm<sup>9</sup> with independent variable equal to the square of the distance. In this way the taking of square roots is avoided. The equations of motion are numerically integrated with a simple second-difference formula and a time step of  $1.0 \times 10^{-14}$  s, chosen as the best compromise between numerical stability and precision. The stability of the temperature, calculated from the mean square velocity, was taken to be an indication of equilibrium and of the performance of the algorithm. Equilibrium data were collected and saved after the system had evolved for several thousand time steps. Data pertinent to the line shape problem, active atom velocities, and the difference potential matrix [Eq. (6)] were saved for 16384 time steps.

The molecular-dynamics simulation gives the time-dependent difference potential matrix in a representation that moves with the sodium atom,

but is orientationally space fixed. In this work we focus on the applicability of the molecular-dynamics method to the optical line-shape problem and on the effect of perturber-perturber interactions on the line shape in a high pressure gas. To this end we analyze the molecular-dynamics data to simulate a system which evolves adiabatically along a classical path with spin-orbit coupling and Doppler broadening both neglected. The data are analyzed in three ways.

The first analysis is made to evaluate the performance of the molecular-dynamics technique and the importance of perturber-perturber interactions for a simplified physical model to which the Anderson-Talman theory<sup>6</sup> (Sec. IV) can be applied in an unambiguous manner. This analysis is unrealistic in that it utilizes a single diatomic excited state potential and simple pairwise additivity, and thus ignores the degeneracy of the atomic excited state. The second analysis uses the three polyatomic excited-state adiabatic potential surfaces for the interaction of the degenerate atom with the perturbers, and the third analysis, the most realistic, includes the vector transition moment, and thus accounts for the effects of relaxation of polarization.<sup>2</sup>

In the first analysis, a single upper-state potential, the  $A^2\Pi$  or  $B^2\Sigma$ , is used. The corresponding difference potential yields an instantaneous frequency  $\nu_\Pi$  or  $\nu_\Sigma$ . In terms of the difference potential matrix [Eq. (2)]

$$h\nu_\Pi = \bar{V} + \text{Tr}\underline{G} \quad (8)$$

and

$$h\nu_\Sigma = \bar{V} - \text{Tr}\underline{G}. \quad (9)$$

All frequencies are measured relative to the unperturbed atomic line. Then the phase of the radiation

$$\phi(t) = 2\pi \int_0^t \nu(t') dt', \quad (10)$$

where the subscript  $\Sigma$  or  $\Pi$  has been omitted.

The signal

$$f(t) = \begin{cases} |\mu| \exp[i\phi(t)], & 0 \leq t \leq T \\ 0, & t < 0; t > T \end{cases} \quad (11)$$

where  $T$  is the duration of the simulation, is Fourier transformed<sup>10</sup> (FT)

$$F(\nu) = \text{FT}^{-1}[f(t)] \equiv \int_{-\infty}^{\infty} \exp(-2\pi i\nu t) f(t) dt \quad (12)$$

and squared to give the line shape

$$\text{Re}I(\nu) = F^*(\nu)F(\nu), \quad (13)$$

which must, however, be treated further to reduce noise due to statistical fluctuations. The line

shape is Fourier transformed to give the autocorrelation function

$$C(\tau) = \text{FT}^+[I(\nu)] \equiv \int_{-\infty}^{\infty} \exp(2\pi i\nu\tau) \text{Re}I(\nu) d\nu. \quad (14)$$

The correlation function so obtained extends for the full time range, 16 384 time steps, but the later times contribute only noise. A window is used to select the statistically significant data and discard the noise. The autocorrelation function [Eq. (14)] is multiplied by a window function<sup>11</sup>:

$$w(\tau) = \begin{cases} \pi^{-1} |\sin(\pi\tau/M)| + (1 - |\tau|/M) \cos(\pi\tau/M), & |\tau| \leq M \\ 0, & |\tau| > M \end{cases} \quad (15)$$

and extended to negative times by the relation  $C(-\tau) = C^*(\tau)$ , so that the Fourier transform will give only the real part of the line-shape function  $I(\nu)$ ,

$$\text{Re}I(\nu) = \text{FT}^{-1}[C(\tau)]. \quad (16)$$

In this way, the noise is reduced to an acceptable level while good resolution is retained if  $M$  is chosen to be 128 time steps, the value used to give the line shapes shown here. A value of  $M = 256$  gives a line shape indistinguishable, except for a minor increase in noise, from that given by  $M = 128$ , so the results are rather insensitive to the choice of the size of the window.

In the second analysis, the adiabatic approximation with scalar transition moment, the difference potential is diagonalized<sup>12</sup> at each time step

$$h\underline{\nu} = \underline{D}^T \underline{\Delta} \underline{V} \underline{D}, \quad (17)$$

to give the time-dependent frequencies  $\nu_j$ ,  $j = 1, 2, 3$ . From here the analysis follows the preceding one with  $\nu_j$  replacing  $\nu$  in Eq. (10) and with the correlation functions averaged

$$C(\tau) = \frac{1}{3} \sum_{j=1}^3 C_j(\tau) \quad (18)$$

before the window is applied.

In the last and most realistic analysis, the vector properties of the transition moment are considered. The components of the eigenvector matrix of the difference potential are proportional to the Cartesian components of the transition moment (Sec. II). Thus, Eq. (11) is replaced by

$$f_{ij}(t) = |\mu| D_{ij}(t) \exp[i\phi_j(t)] \quad (19)$$

and

$$C(\tau) = \frac{1}{3} \sum_{i=1}^3 \sum_{j=1}^3 C_{ij}(\tau). \quad (20)$$

Otherwise the analysis is identical to the first two. Since the phases of the eigenvectors [Eq.

(17)] are necessarily arbitrary, any numerical method for determining them may introduce noise from random sign changes. This is eliminated by a simple test to insure that the scalar product of the eigenvectors at two successive time steps is nearer +1 than -1.

#### IV. CLASSICAL PATH ANDERSON-TALMAN THEORY

Following Royer,<sup>1</sup> we write the Anderson-Talman theory<sup>6</sup> autocorrelation function as an exponential

$$C(\tau) = C(0)\exp[G_1(\tau)], \quad (21)$$

where

$$G_1(\tau) = n[C_1(\tau) - C_1(0)]/I_0. \quad (22)$$

Here  $n$  is the number density of perturbers,  $C_1(\tau)$  is the one-perturber dipole autocorrelation function, and  $I_0$  is the atomic line strength. By means of Eqs. (16), (21), and (22) the density-dependent line shape is expressed in terms of the one-perturber autocorrelation function.

The one-perturber autocorrelation function cannot, however, be obtained as a simple Fourier transform of the one-perturber line shape. The function  $C_1(\tau)$  does not approach zero, but becomes a linear function of time, as the time  $\tau$  approaches infinity. This fact, which results from the physical approximation of one perturber in an infinite volume, leads to the divergence of Fourier integrals over the one-perturber line shape.

It is possible to evaluate  $C_1(\tau)$  while avoiding divergent integrals if the second time derivative  $\ddot{C}_1(\tau)$ , which is Fourier transformable, is evaluated and then integrated twice. The second derivative is determined by

$$\ddot{C}_1(\tau) = -4\pi^2 \text{FT}^*[\nu^2 I_1(\nu)], \quad (23)$$

where  $I_1(\nu)$  is the one-perturber line shape and  $\nu^2 I_1(\nu)$  is finite everywhere. Then, from Eq. (22),

$$G_1(\tau) = (n/I_0) \left( \int_0^\tau \int_0^t \ddot{C}_1(s) ds dt + \dot{C}_1(0)\tau \right). \quad (24)$$

For the purposes of numerical evaluation, the iterated integral is converted to a single integral

$$G_1(\tau) = (n/I_0) \left( \int_0^\tau (\tau - t) \ddot{C}_1(t) dt + \dot{C}_1(0)\tau \right). \quad (25)$$

The value of  $\dot{C}_1(0)$  is purely imaginary and is related to the first moment of the one-perturber line shape

$$\dot{C}_1(0) = 2\pi i \int_{-\infty}^{\infty} \nu I_1(\nu) d\nu. \quad (26)$$

When  $\nu^2 I_1(\nu)$  and  $\dot{C}_1(0)$  have been calculated, either by quantum mechanical or classical path methods, Eqs. (23), (25), (21), and (16) are readily evaluated to yield the density-dependent line shape. For

consistency with the molecular-dynamics calculations, a classical path method is used here. In the description, which follows, the notation

$$[Z(J, E_a)]_{\text{av}} = Q_T^{-1} \int dE_a \exp\left(\frac{-E_a}{kT}\right) \sum_J (2J+1) Z(J, E_a) \quad (27)$$

is used. Here

$$Q_T = (2\pi\mu kT/\hbar^2)^{3/2} \quad (28)$$

and  $\mu$  is the reduced mass of the diatom. In some of the calculations an average over diatomic states that correlate with degenerate atomic states is also performed. Then Eq. (27) is multiplied by the statistical weight and summed over diatomic states.

In the classical path formulation of the one-perturber problem, the fundamental quantity is the time-dependent signal

$$f(t) = \begin{cases} \mu(R(t)) \exp\left(\frac{i}{\hbar} \int_0^t \Delta V[R(t')] dt'\right), & t \geq 0 \\ 0, & t < 0 \end{cases} \quad (29)$$

where  $R(t)$  is the trajectory in the initial state potential. The function  $C_1(\tau)$  is related to the autocorrelation function of the signal  $f(t)$ :

$$C_1(\tau) = \frac{1}{\pi\hbar} \left( \int_0^\infty f^*(t) f(t+\tau) dt \right)_{\text{av}} \quad (30)$$

and

$$\dot{C}_1(0) = \frac{1}{\pi\hbar} \left( \int_0^\infty f^*(t) \dot{f}(t) dt \right)_{\text{av}}. \quad (31)$$

Explicitly, if it is assumed that  $\mu(R)$  is a slowly varying function,

$$\dot{C}_1(0) = \frac{i}{\pi\hbar^2} \left( \int_0^\infty \mu^2(R) \Delta V(R) dt \right)_{\text{av}}. \quad (32)$$

The classical path evaluation of  $\nu^2 I_1(\nu)$  is derived by writing

$$\nu^2 I_1(\nu) = (4\pi^3\hbar)^{-1} [-2\pi i \nu F^*(\nu) 2\pi i \nu F(\nu)]_{\text{av}}, \quad (33)$$

where

$$2\pi i \nu F(\nu) = \text{FT}^{-1}[\dot{f}(t)], \quad (34)$$

and

$$\dot{f}(t) = \begin{cases} (i/\hbar) \mu(R(t)) \Delta V(R(t)) \exp\left(\frac{i}{\hbar} \int_0^t \Delta V(R(t')) dt'\right), & t \geq 0 \\ 0, & t < 0. \end{cases} \quad (35)$$

It has again been assumed that  $\mu(R)$  is a slowly varying function.

Note that the required Fourier transforms of Eqs. (34), (23), and (16) are all well behaved. The function  $f(t)$  approaches zero for large times due to the  $\Delta V$  factor. The function  $\nu^2 I_1(\nu)$  remains

finite as  $\nu \rightarrow 0$ . The function  $C(\tau)$  approaches zero for large time because the real part of  $G_1(\tau)$  [Eq. (22)] becomes large and negative at large times. Therefore, a stable numerical algorithm is achieved.

The algorithm is in two parts. In the first part  $\nu^2 I_1(\nu)$  and  $\hat{C}_1(0)$  are evaluated. In the average over collision energies, Laguerre-Gauss integration is used, while a simple sum is used for the angular momentum. Twelve Laguerre points are used in the energy integration. It is usually unnecessary to sum over each value of  $J$  in order to achieve the desired accuracy (3 or 4 significant figures). For the NaAr system every fifth  $J$  value was used.

For each  $J$  and  $E$ , a classical (curved) trajectory is determined by means of a second-order Runge-Kutta method<sup>13</sup> with a constant time step. A rather small time step is necessary for the fast-Fourier transform steps to come later, so high-order integration methods for the other steps in the calculation are not practical. For each trajectory, the time derivative of the signal [Eq. (35)] is evaluated, Fourier transformed, and squared to give a contribution to the average of Eq. (33). The phase integral in Eq. (35) is evaluated with simple trapezoidal rule integration and the "fast-Fourier transform"<sup>10</sup> is used. Sufficient accuracy has been achieved with 2048 time steps of 100 a.u. duration (1 a.u. of time =  $2.41888 \times 10^{-17}$  s). The computer time required for a complete one-perturber spectrum is about 1 h on a CDC CYBER 70/71 computer.

The efficiency of this algorithm, as compared to others,<sup>14-17</sup> is due to the elimination of an explicit evaluation of the autocorrelation function. The fast-Fourier transform is used to change to the frequency domain where a simple square of the signal is evaluated. The Fourier transform is made possible because the spectrum is expressed in terms of the time derivative of the signal  $\dot{f}(t)$ , which is a well-behaved function.

In the second part of the algorithm the quantity  $\nu^2 I_1(\nu)$  is backtransformed to give  $C_1(\tau)$  [Eq. (23)]. The time integral of Eq. (25) is done by trapezoidal rule integration. Finally, the result is multiplied by the density [Eq. (22)], exponentiated [Eq. (21)], and transformed [Eq. (16)] to give the line shape. Only seconds of computer time is required for the second part of the algorithm.

## V. RESULTS

Molecular-dynamics and Anderson-Talman (AT) calculations of the shape of the resonance line of sodium perturbed by argon were carried out with the methods described above and using

NaAr pair potentials for the ground and excited states interpolated from the configuration interaction results of Saxon, Olson, and Liu.<sup>18</sup> The  $\text{Ar}_2$  interaction was that derived from experimental bulk property data by Barker, Fisher, and Watts.<sup>19</sup> A temperature of 450 K and a density of  $2 \times 10^{21} \text{ cm}^{-3}$  (r.d. = 74.4) were used. Under these conditions Doppler broadening is negligible, and the spin-orbit splitting is small compared to the linewidth. Neither is included here.

In the first set of calculations, the molecular-dynamics data are analyzed and the AT calculation is done with the assumption of a single diatomic excited-state potential, either the  $\Sigma$  or the  $\Pi$ . In this case there are no ambiguities in the application or interpretation of the Anderson-Talman theory. The many-body line shape is simply a sum of convolutions of one-perturber line shapes. The spectra are compared in Figs. 1 and 2. Within statistical error the spectra are identical. This result indicates that the molecular-dynamics method can be applied to the atomic-line-shape problem, that the AT concept is good for nondegenerate states up to the relatively high density

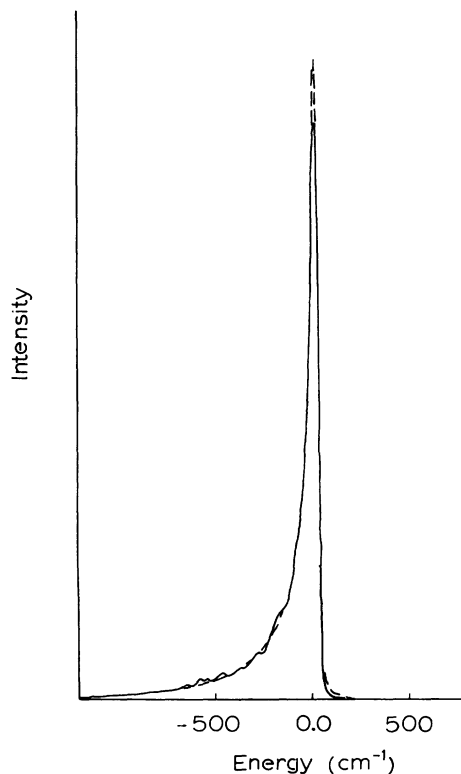


FIG. 1. Comparison of Anderson-Talman (AT) and molecular-dynamics (MD) line shapes for a single upper  $\Pi$ -state potential. The intensity is relative, but the spectra are normalized to have the same integrated intensity. AT----; MD—.

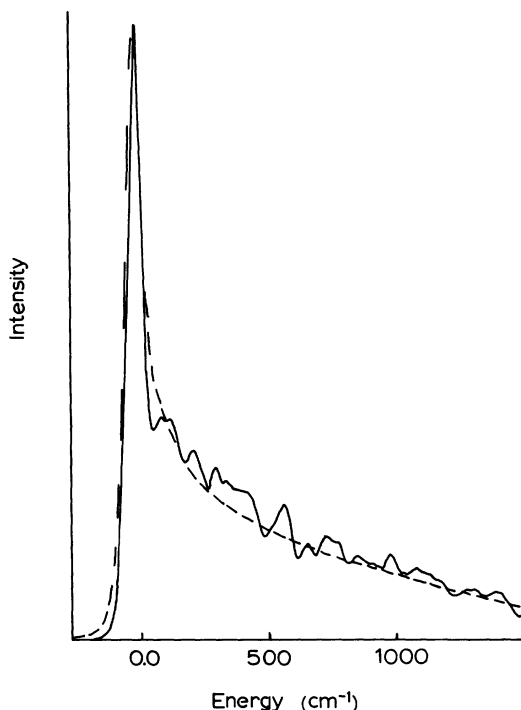


FIG. 2. Comparison of AT and MD line shapes for a single upper  $\Sigma$ -state potential. AT----; MD—.

used here, and that the line shape is insensitive to the perturber-perturber interactions at this density. With the assumption of pairwise additivity of interaction potentials, the perturber-perturber interactions influence the trajectory in the molecular-dynamics simulation, but they cancel in the difference potential. It is because the line shape is sensitive to the difference potential, but relatively insensitive to the details of the trajectory, that the perturber-perturber interactions are unimportant. We note in passing that the  $A^2\Pi-X^2\Sigma$  difference potential is uniformly negative, whereas the  $B^2\Sigma-X^2\Sigma$  difference potential is predominantly positive; thus, the  $\Pi$  state leads to a line shape with no blue wing and the  $\Sigma$  state to one with no extended red wing.

The dipole autocorrelation functions from the molecular dynamics and AT calculations for the single difference potential cases are compared in Figs. 3 and 4. The autocorrelation functions are very similar, however, there are deviations at longer times that appear to be systematic and larger than statistical error.

In an allowed atomic transition at least one of the states involved must be degenerate and therefore correlate with more than one molecular state of the system, active atom plus perturbers. When adding diatomic interactions to estimate the polyatomic energy surface these must be added in the

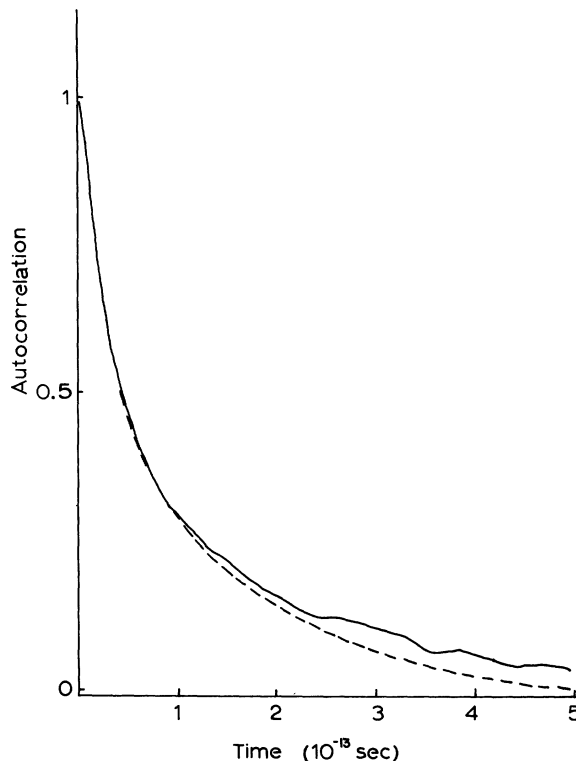


FIG. 3. Comparison of AT and MD autocorrelation functions for a single upper  $\Pi$ -state potential. AT----; MD—.

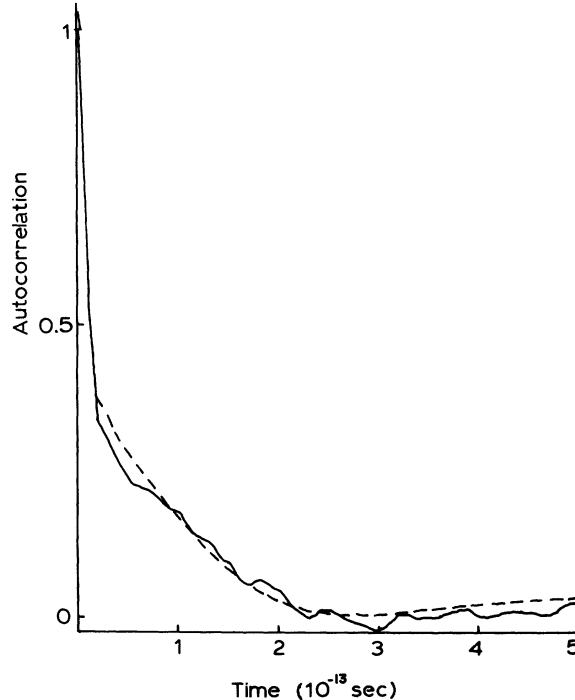


FIG. 4. Comparison of AT and MD autocorrelation functions for a single upper  $\Sigma$ -state potential. AT----; MD—.

same space-fixed representation. This leads to a difference potential matrix for the system. An adiabatic approximation to the molecular-dynamics line shape is determined by diagonalizing this potential matrix and adding the spectra calculated from the use of each eigenvalue. In the low density limit, when only one perturber is interacting with the active atom at one time, the eigenvalues are the values of the adiabatic diatomic interaction potentials. For the NaAr case there are three eigenvalues, one of which approaches the  $\Sigma$ -state energy at low densities while the other two approach the  $\Pi$ -state energy. There is no AT-like approximation that is strictly analogous to the molecular-dynamics adiabatic approximation, but there are two plausible approximations, both of which approach the correct form in the limit of low densities. One approximation is simply to add the single state  $N$ -perturber spectra (with the appropriate statistical weights); the other is to add the one-perturber spectra for the  $\Sigma$  and  $\Pi$  states.

In Fig. 5 the sum of the AT  $N$ -perturber spectra for the  $\Sigma$  and  $\Pi$  states is compared to the adiabatic molecular-dynamics line shape. The agreement is poor. The reason is that the three components of the adiabatic molecular-dynamics line shape,

the spectra calculated from each of the three eigenvalues, do not look like one  $\Sigma$ -state spectrum and two  $\Pi$ -state spectra (Figs. 6-8). The greatest discrepancy is found in the spectrum from the second eigenvalue which resembles neither the  $\Sigma$ - nor the  $\Pi$ -state spectrum.

When the sum of the  $\Sigma$ - and  $\Pi$ -state one-perturber spectra (with statistical weights of  $\frac{1}{3}$  and  $\frac{2}{3}$ ) is used in Eq. (23), the resulting AT  $N$ -perturber spectrum is in excellent agreement with the adiabatic molecular-dynamics line shape (Fig. 9).

It is possible to incorporate the rotation of the transition dipole moment for each molecular transition (active atom plus perturbers) into the adiabatic molecular-dynamics line shape [Eq. (20)]. In Fig. 10 the effect of the rotation of the direction of polarization is assessed by comparing the results of molecular-dynamics analyses with and without consideration of polarization. The rotation of the polarization axis is seen to have a slight broadening effect on the center of the line. This is reflected in a modified decay rate in the auto-correlation function (Fig. 11).

## VI. DISCUSSION

The molecular-dynamics technique has been shown to be a useful tool for studying the dynamic processes involved in the formation of the shapes of pressure-broadened atomic spectral lines.

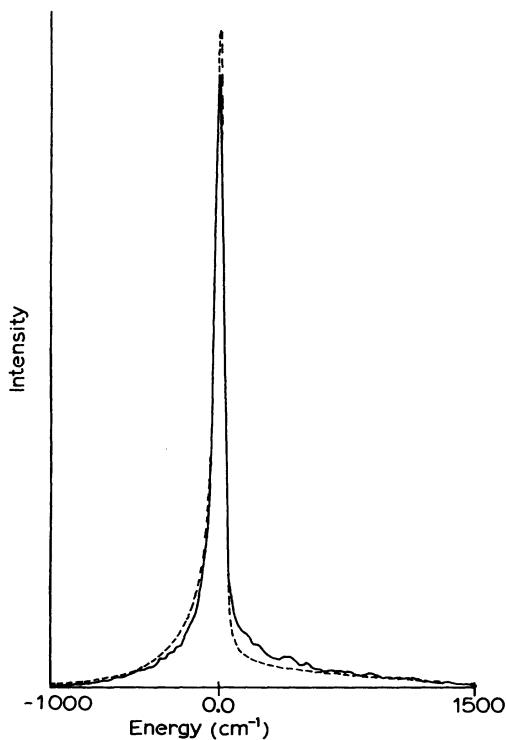


FIG. 5. Comparison of weighted average of AT line shapes for  $\Pi$  and  $\Sigma$  states with adiabatic MD line shape. AT----; MD—.

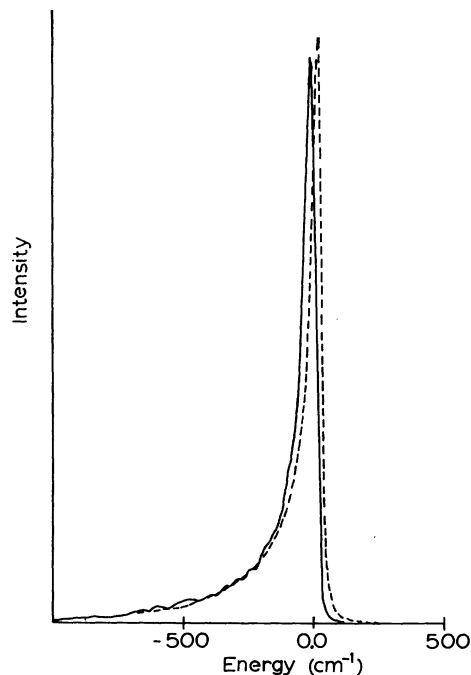


FIG. 6. Comparison of AT line shape for a single upper  $\Pi$ -state potential with MD line shape from first eigenvalue of difference potential. AT----; MD—.

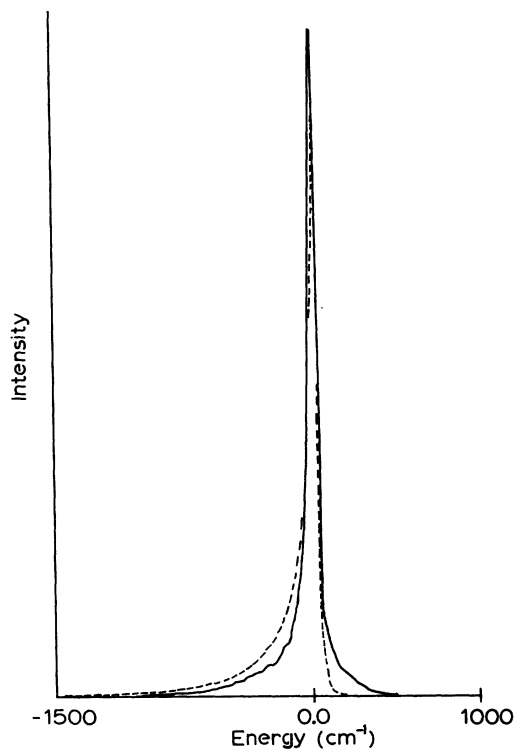


FIG. 7. Comparison of AT line shape for a single upper  $\Pi$ -state potential with MD line shape from second eigenvalue of difference potential. AT----; MD—.

Even though there is only one active atom in the system, along with 255 perturbers, the statistical error in the calculated spectrum is held to an acceptable level with molecular-dynamics runs of

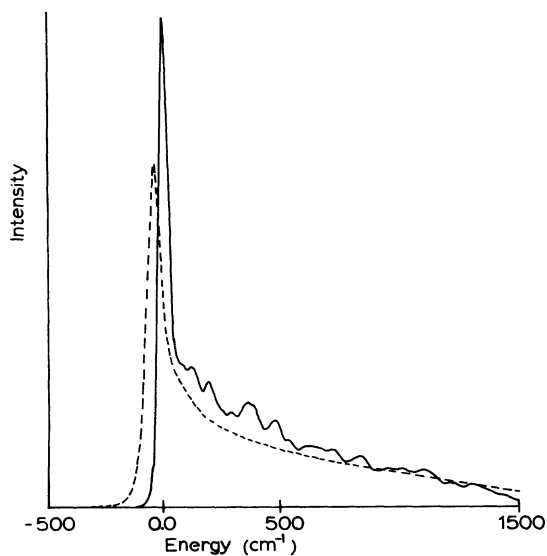


FIG. 8. Comparison of AT line shape for a single upper  $\Sigma$ -state potential with MD line shape from third eigenvalue of difference potential. AT----; MD—.

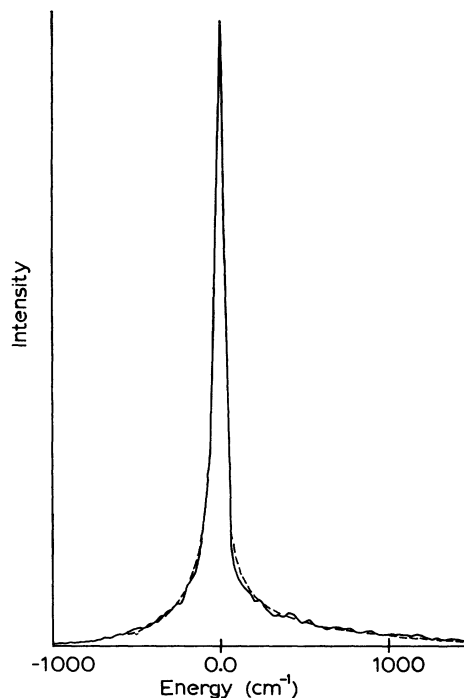


FIG. 9. Comparison of AT line shape calculated from weighted average of  $\Pi$ - and  $\Sigma$ -state one-perturber spectra with adiabatic MD line shape. AT----; MD—.

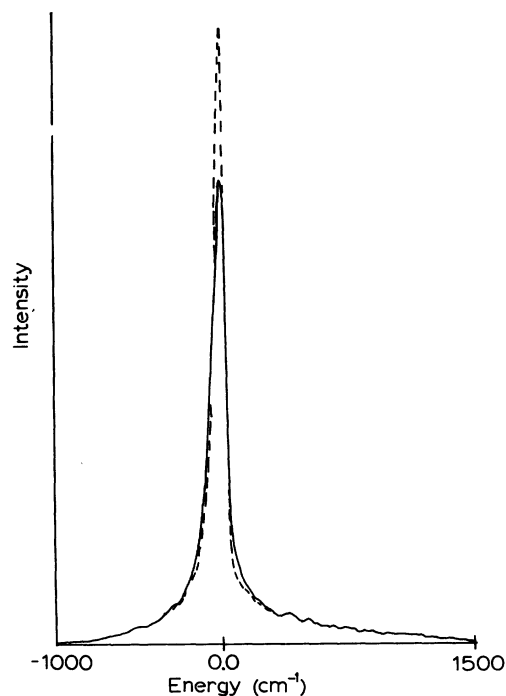


FIG. 10. Comparison of adiabatic MD line shape with the adiabatic MD line shape that incorporates relaxation of polarization. No polarization----; With polarization—.



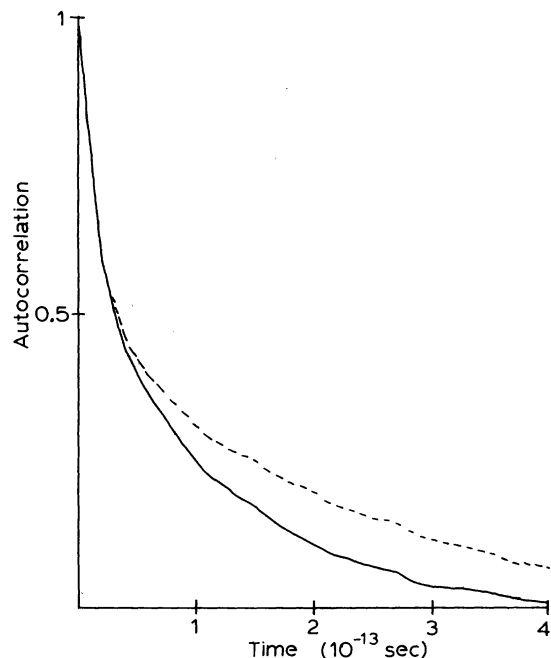


FIG. 11. Comparison of adiabatic MD autocorrelation function with the adiabatic MD autocorrelation function that incorporates relaxation of polarization. No polarization----; With polarization—.

a readily attainable length (less than 20 000 time steps). The consistency found between the molecular-dynamics and the Anderson-Talman theory results confirms the utility of the molecular-dynamics approach and shows for one system (sodium perturbed by argon,  $T = 450$  K,  $N = 2 \times 10^{21}$   $\text{cm}^{-3}$ ) that the basic assumptions of the Anderson-Talman theory are remarkably good. The effects of coupling between atomic states, the spin-orbit interaction, and Doppler broadening are expected to be small corrections to the line shape at this high pressure, and have been neglected for simplicity. Extensions to investigate the importance of these more subtle effects will be pursued in future work.

The remarkable agreement between the Anderson-Talman theory and the molecular-dynamics spectra for the simple nondegenerate case (single upper-state potential) indicates that the independent-perturber approximation inherent in the theory is valid, even at the rather high density used here. There is a noticeable discrepancy in the long-time tail of the autocorrelation function when the  $\Pi$ -state interaction is used, but this causes only a very small difference in the spectra.

When the degeneracy of the excited state, and therefore the difference potential matrix, is con-

sidered in an adiabatic approximation, the Anderson-Talman theory still gives a line shape in excellent agreement with that from the simulation (Fig. 9) provided that the one-perturber spectrum is constructed by adding the contributions from the  $\Sigma$  and  $\Pi$  states before the density dependence is introduced; that is, when the spectra are added at the "one-perturber level." The meaning of this result is clear if we decompose Eq. (21):

$$C(\tau) = C(0) \exp[G_{I\Sigma}(\tau)] \exp[2G_{I\Pi}(\tau)]. \quad (36)$$

The  $\Sigma$ - and  $\Pi$ -state autocorrelation functions are multiplied to give the density-dependent autocorrelation function, which is equivalent to convoluting the corresponding spectra.

In the molecular-dynamics simulation, the difference potentials are considered to be pairwise additive as matrices in a space-fixed representation. Thus, as long as the matrix representation is retained, the effects of two different perturbers are correlated only by means of the perturber-perturber interactions, which have already been shown to be unimportant for our system. However, when the difference potential is diagonalized to form the adiabatic approximation, a different kind of correlation of perturber effects arises. For simplicity, consider the two perturber case and let the positions of the sodium atom and one of the argon atoms be fixed. As the second perturber approaches the Na-Ar pair, each of three eigenvalues will receive a contribution from the approaching argon atom, however, that contribution may be from a  $\Pi$ -state interaction, a  $\Sigma$ -state interaction, or a combination thereof, depending upon the position of the first perturber. The agreement found between the AT and molecular-dynamics spectra indicates that this correlation is also unimportant for our system. Within the molecular-dynamics framework, the adiabatic approximation is expected to be good, an assertion that will be tested in future work, thus the Anderson-Talman theory with adiabatic diatomic interactions, although not a rigorous counterpart to the  $N$ -body adiabatic approximation, should be reliable for predicting the shapes of atomic lines at high perturber densities.

The vector properties of the transition moment make possible a broadening mechanism for atomic lines that involves relaxation of polarization. A quantitative assessment of the importance of this mechanism is readily obtained from the adiabatic molecular-dynamics method, since an eigenvector of the difference potential matrix is proportional to the transition moment for the corresponding state. For our system the effect is noticeable (Figs. 10 and 11), but it is less important than energy changing effects.

Better agreement between the Anderson-Talman theory and molecular-dynamics line shapes is reported here, than was indicated in preliminary reports<sup>20,21</sup> of this work. The reason is that better numerical methods have been used here.

## ACKNOWLEDGMENTS

This work was partly supported by the National Science Foundation. Computer time was provided by the Graduate College of the University of Iowa.

- 
- <sup>1</sup>A. Royer, *Can. J. Phys.* **52**, 1816 (1974).  
<sup>2</sup>F. Schuller and W. Behmenburg, *Phys. Rep. C* **12**, 273 (1974).  
<sup>3</sup>B. J. Alder and T. E. Wainwright, *J. Chem. Phys.* **31**, 459 (1959).  
<sup>4</sup>J. M. Hailein, *Computer Modeling of Matter*, ACS Symposium Series, edited by P. Lykos (American Chemical Society, Washington, 1978), Vol. 86.  
<sup>5</sup>A. Jablonski, *Phys. Rev.* **68**, 78 (1945).  
<sup>6</sup>P. W. Anderson, *Phys. Rev.* **86**, 809 (1952); P. W. Anderson and J. D. Talman, *Bell Teleph. Syst. Tech. Publ. No.* 3117.  
<sup>7</sup>K. M. Sando, G. J. Erickson, and R. C. Binning, Jr., *J. Phys. B* **12**, 2697 (1979).  
<sup>8</sup>R. W. Hockney, S. P. Goel, and J. W. Eastwood, *J. Comp. Phys.* **14**, 148 (1974).  
<sup>9</sup>The tension-spline computer code written by K. Kaiser at Argonne National Laboratory was used.  
<sup>10</sup>The fast-Fourier transform developed by J. W. Cooley and J. W. Tukey, *Math. Comput.* **19**, 297 (1965) was used throughout. Two computer codes based upon this algorithm were used: A locally written code obtained from the University of Iowa Weeg Computer Center; and a code published in R. C. Singleton, *IEEE Trans. Audio and Electroacoust.* **AU-15**, 91 (1967).  
<sup>11</sup>A. Papoulis, *IEEE Trans. Inf. Theory* **IT-19**, 9 (1973).  
<sup>12</sup>Eigenvalues and eigenvectors were determined with the subroutine EIGRS from the IMSL library, International Mathematical & Statistical Libraries, Inc. Houston, Texas.  
<sup>13</sup>P.-J. Davis and I. Polonsky, in *Handbook of Mathematical Functions*, edited by M. Abramowitz and I. A. Stegun (U. S. GPO, Washington, D. C., 1964), Appl. Math. Ser. 55.  
<sup>14</sup>M. Takeo, *Phys. Rev. A* **1**, 1143 (1970).  
<sup>15</sup>A. K. Atakan and H. C. Jacobson, *Phys. Rev. A* **7**, 1452 (1973).  
<sup>16</sup>N. F. Allard, S. Sahal-Brechot, and Y. G. Biraud, *J. Phys. B* **7**, 2158 (1974).  
<sup>17</sup>J. F. Kielkopf, *J. Phys. B* **9**, 1601 (1976).  
<sup>18</sup>R. P. Saxon, R. E. Olson, and B. Liu, *J. Chem. Phys.* **67**, 2692 (1977).  
<sup>19</sup>J. A. Barker, R. A. Fisher, and R. O. Watts, *Mol. Phys.* **21**, 657 (1971).  
<sup>20</sup>G. J. Erickson and K. M. Sando, Abstracts of the 4th Int'l. Conference on Spectral Line Shapes, Windsor, Ontario, 1978 (unpublished).  
<sup>21</sup>G. J. Erickson and K. M. Sando, Abstract of the Division of Electron and Atomic Physics Meeting of the American Physical Society, Houston, Texas, 1979 (unpublished).